Sound Propagation through Circular Ducts with Spiral Element Inside

Wojciech Łapka*
Division of Vibroacoustics and System Biodynamics, Institute of Applied Mechanics,
Poznań University of Technology, Poland.
*Corresponding author: W. Łapka, Piotrowo 3 Street, 60-965 Poznań, Poland. Wojciech.Lapka@put.poznan.pl

Abstract: This paper examines a sound propagation without airflow through circular ducts with spiral element inside. Models are numerically computed in three-dimensions. The spiral element in duct is a newly analyzed acoustical element, geometrically similar to the well-known Archimedes screw. Significantly it can be applied in ducted systems, such as ventilation, air-conditioning and heat systems. This practical modification can improve a sound attenuation performance in specified band of frequency. The paper introduces the most important properties of this solution.

Keywords: acoustics**,** sound propagation, spiral duct, sound attenuation.

1. Introduction

One of the most important areas of acoustics [1], is sound propagation in ducts and mufflers [2]. Another topic of considerable interest is the case of curved ducts [3-5]. Early stage research problem, partially investigated in this paper, is sound propagation in spiral ducts [6-11]. This solution (Fig. 1b) is similar to the well known Archimedes screw (Fig.1a), historically used for transferring water from a low-lying body of water into irrigation ditches.

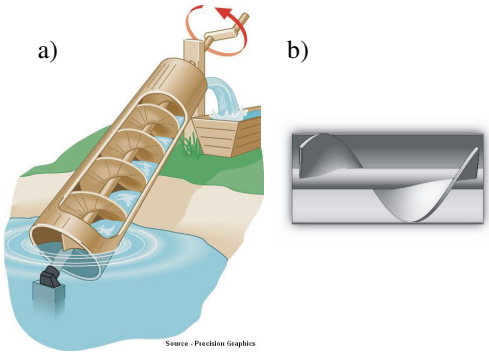

Figure 1. Archimedes screw (a) and one spiral turn of the spiral duct (b).

In several papers [6-11] acoustical properties of spiral ducts are numerically computed in a COMSOL Multiphysics computer application [12]. There are presented the acoustical attenuation performance parameters [2], such as the transmission loss (TL) [6,9,10], the noise reduction (NR) [8], and the insertion loss (IL) [11]. Hence, it's already proven that inserting just one spiral turn at the inlet circular duct of the round silencer can improve the sound attenuation performance of this silencing system [6].

Obviously, the higher acoustical parameters are achieved when the spiral duct has more eligible geometrical parameters fitted to the sound wave length. In that case can be observed the highest TL at a resonance frequency of the spiral duct – Fig.2., which produce phenomenal sound pressure level (SPL) distribution at the outlet – Fig.3.

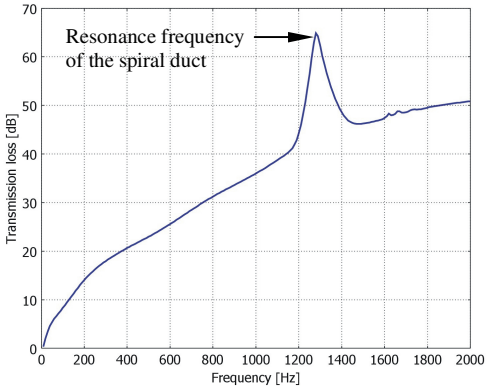

Figure 2. Transmission loss of the round silencer with one spiral turn of the spiral duct at the inlet.

In reference [9] can be found a comparison between the well known acoustic band stop filter (BSF) - Helmholtz resonator [13-16] and spiral duct. Here the spiral duct can be found as an alternative solution in ducted systems, when Helmholtz resonators do not work effectively. The newest paper [7] shows a good agreement between experimental and numerical results of the sound pressure level distribution at the outlet of the spiral duct. Presented validation is a very important information, because it gives a very high applicable potential for spiral ducts.

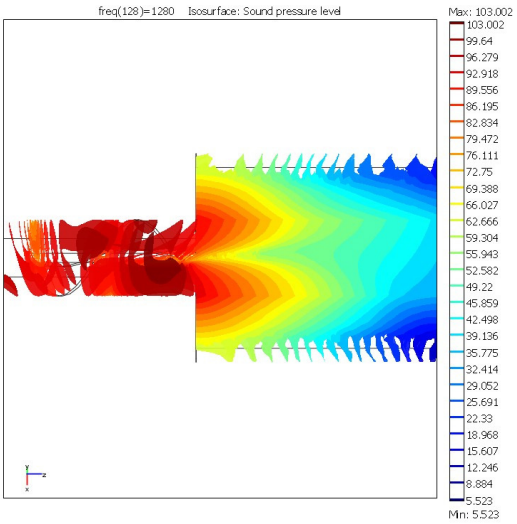

Figure 3. Sound pressure level distribution at the resonance frequency of one spiral turn of the spiral duct placed at the inlet of the round silencer.

On this basis, as described above, this paper consider a sound propagation through circular ducts with spiral element inside.

2. General assumptions

Three dimensional (3D) sound propagation without air flow in circular ducts with spiral element inside is numerically calculated by the use of COMSOL Multiphysics computer application [12]. Only transmission loss (TL) as an acoustical filter performance parameter [2] is measured and in terms of the progressive wave components can be expressed as:

$$TL = 10\log_{10}\left|\frac{S_n A_n^2}{2}\frac{2}{S_1 A_1^2}\right|, \qquad B_1 = 0 \quad (1)$$

$$= 20\log_{10}\left|\frac{A_n}{A_1}\right|, \qquad B_1 = 0. \quad (2)$$

Here S_n and S_1 denotes the cross-section areas of the exhaust pipe and tail pipe, respectively, which are equal in the experiments for transmission loss. A_n and A_1 are the incident (in the exhaust pipe) and transmitted (in the tail pipe) wave pressures, respectively. B_1 denotes the reflected wave pressure in the tail pipe. The anechoic termination ensures B_1=0 (see Fig.4). However, experimentally A_n cannot be measured in isolation from the reflected wave pressure B_n, computationally there is no difficulty.

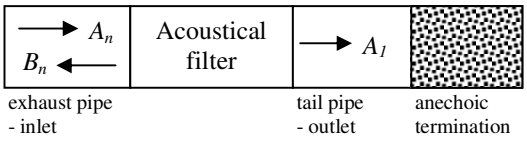

Figure 4. Definition of transmission loss: $TL=20\log_{10}|A_n/A_1|$.

The walls of the circular ducts and the spiral elements are acoustically hard. There isn't any absorptive material inside.

3. Model definition, equations and boundary conditions

Dimensions of the spiral elements (see Fig.5) are connected with circular ducts dimensions by a specific parameters given by relation of a spiral lead s, a thickness of a spiral profile g, and cylindrical mandrel diameter d_m to a constant circular duct diameter d and are presented as s/d, g/d and d_m/d ratio, respectively.

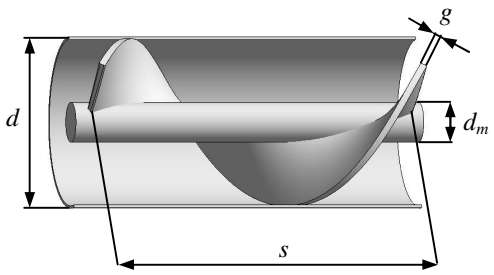

Figure 5. Dimensions of the circular duct and spiral element.

The problem is solved in the frequency domain using the time-harmonic Pressure Acoustics application mode [12]. The final solving parameter is the acoustic pressure p [Pa], which can be computed by the use of slightly modified Helmholtz equation:

$$\nabla \cdot \left(-\frac{\nabla p}{\rho_0}\right) - \frac{\omega^2 p}{c_s^2 \rho_0} \quad (3)$$

where ρ_0 is the density of air (ρ_0=1,23 kg/m^3), c_s is the speed of sound in air (c_s=343m/s), and ω gives the angular frequency.

For computational needs, the TL is expressed as the difference between the outgoing power at the outlet w_o and the incoming power at the inlet w_i,

$$TL = 20\log_{10}\left(\frac{w_i}{w_o}\right) \quad (4)$$

Each of component quantities in equation (4) are calculated as an integral over the corresponding surface $\partial\Omega$ of circular ducts cross-sections S_n and S_1:

$$w_i = \int_{\partial\Omega} \frac{p_0}{2\rho_0 c_s} dS \quad (5)$$

$$w_o = \int_{\partial\Omega} \frac{|p_c|}{2\rho_0 c_s} dS \quad (6)$$

where p_0 is the source acoustic pressure at the inlet, [Pa], and p_c is the transmitted acoustic pressure at the outlet, [Pa].

The boundary conditions are of three types [12]. Acoustically hard walls at the solid boundaries, which are the walls of the spiral element profile, mandrel and circular duct, the model uses sound hard (wall) boundary conditions:

$$\left(\frac{\nabla p}{\rho_0}\right)\cdot \mathbf{n} = 0 \quad (7)$$

The boundary condition at the inlet surface of circular duct is a combination of incoming and outgoing plane waves:

$$\mathbf{n}\cdot\frac{1}{\rho_0}\nabla p + ik\frac{p}{\rho_0} + \frac{i}{2k}\Delta_T p = \\ = \left(\frac{i}{2k}\Delta_T p_0 + (1-(\mathbf{k}\cdot\mathbf{n}))ik\frac{p_0}{\rho_0}\right)e^{-ik(\mathbf{k}\cdot\mathbf{r})} \quad (8)$$

where Δ_T denotes the boundary tangential Laplace operator, $k=\omega/c_s$ is the wave number, $\mathbf{n}$ is the natural direction vector for investigated circular duct, and wave vector is defined as $\mathbf{k}=k\mathbf{n}_\mathbf{k}$, where $\mathbf{n}_\mathbf{k}$ is the wave-direction vector. In equation (8), p_0 represents the applied outer pressure, and i denotes the imaginary unit [17]. The inlet boundary condition is valid as long as the frequency is kept below the cutoff frequency for the second propagating mode in the cylindrical duct.

At the outlet boundary is set as the radiation boundary condition which allows an outgoing wave to leave the modeling domain with no or minimal reflections:

$$\mathbf{n}\cdot\frac{1}{\rho_0}\nabla p + i\frac{k}{\rho_0}p + \frac{i}{2k}\Delta_T p = 0 \quad (9)$$

The numerical model is computed by the use of finite element method (FEM) by the terms of the element size [18] and maximum element size equals h_e=0,2(c_s/f_{max}), where f_{max} is the value of maximum investigated frequency (in this paper f_{max}=2kHz). The longitudinal dimension of circular ducts is calculated as infinite by the use of radiation boundary conditions.

4. Results and discussion

The results are presented as the TL[dB] in different frequency ranges. First range is from 10Hz to 2kHz with the computational step of 10Hz, and the second range is from 1kHz to 1,6kHz with the computational step of 1Hz. The spiral element ratios equals: s/d=2, g/d=0,04 and d_m/d=0,24.

Fig. 6 and Fig. 7 shows the TL of the circular duct with spiral element inside for 1st and 2nd frequency range, respectively.

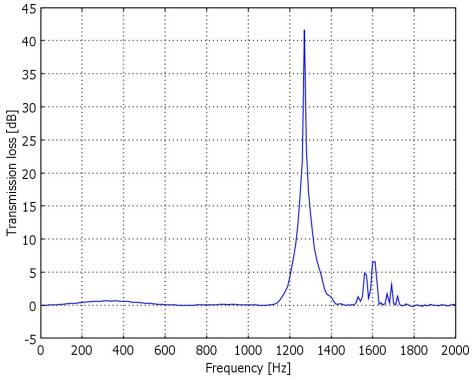

Figure 6. TL of the circular duct with spiral element inside with ratio s/d=2 for a frequency range from 10Hz to 2kHz with the computational step 10Hz.

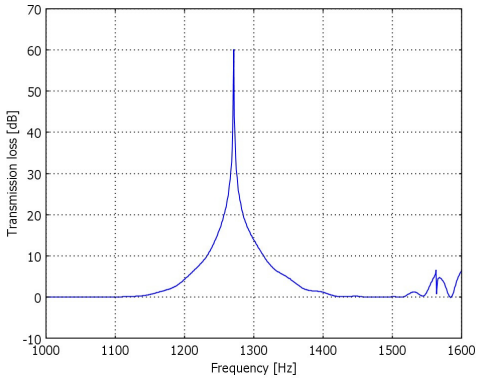

Figure 7. TL of the circular duct with spiral element inside with ratio *s/d*=2 for a frequency range from 1kHz to 1,6kHz with the computational step 1Hz.

Maximum level of TL presented in Fig.6 is about 42dB at the frequency 1270Hz, and by changing computational step to 1Hz in Fig.7, the TL achieves about 60dB at the frequency 1271Hz, which can be recognized as a resonance frequency of the spiral element. In 1st case (Fig.6) it is visible a small growth (about 1dB) of the TL in low frequencies between about 150Hz and 550Hz. In both figures (Fig. 6 and Fig. 7) the sound attenuation considerably increases in a specified frequency range from about 1150Hz to about 1410Hz. This kind of sound attenuation is a well-known property of the acoustical band stop filter – Helmholtz resonator. In both cases there can be observed some variations of TL at frequencies higher than 1550Hz, what can be recognized as the influence of a transverse wave propagation in the circular duct.

Fig. 8 shows the SPL distribution inside investigated model for a resonance frequency 1271Hz of the spiral element. It can be observed that similarly to Fig. 3 the SPLs distribution at the outlet of the spiral element is such that the maximum values of SPL are directed sideways, and the minimum values of SPL are directed in axis of the circular duct. That kind of acoustic wave distribution increases the sound attenuation in a specified band of frequency, which can be determined by the spiral element geometry.

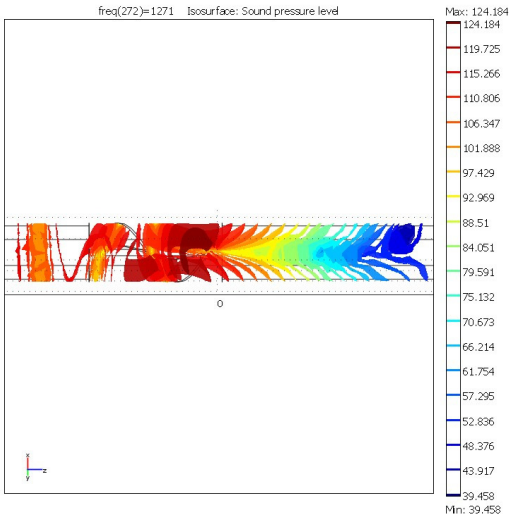

Figure 8. SPL distribution at the resonance frequency 1271Hz of the spiral element inside circular duct.

5. Conclusions

This study introduced the problem of modeling acoustic wave propagation without air flow in spiral shaped elements placed inside circular ducts. Suitable change of dimensions and mutually dependent *s/d*, *g/d* and d_m/d ratios can improve the sound attenuation performance in determined frequency range for any kind of circular duct. Characteristic SPL distribution at the outlet of spiral elements is their property.

Newly discovered acoustical properties of attenuating sound in specified frequency band of spiral elements are a solid base to consider this solution as applicable for industrial systems. It can be applied as an alternative substitution of Helmholtz resonator – well known acoustic band stop filter.

Spiral elements used for attenuating sound in ducted silencing system still need a lot of research work, but already done researches expand a new scientific knowledge in the domain of ducts and mufflers.

6. References

1. Morse P.M., *Vibration and Sound*, 468, McGraw-Hill Book Company Inc., USA, New York (1948)
2. Munjal M.L., *Acoustics of Ducts and Mufflers with Application to Exhaust and Ventilation*

System Design, 328, John Wiley & Sons Inc., Calgary, Canada (1987)
3. Rostafinski W., On the propagation of long waves in curved ducts, *J. Acoust. Soc. Am.*, **52**, 1411-1420 (1972)
4. Rostafinski W., Analysis of propagation of waves of acoustic frequencies in curved ducts, *J. Acoust. Soc. Am.*, **56**, 11-15 (1974)
5. Rostafinski W., Acoustic systems containing curved duct sections, *J. Acoust. Soc. Am.*, **60**, 23-28 (1976)
6. Łapka W., Acoustic attenuation performance of a round silencer with the spiral duct at the inlet, *Archives of Acoustics*, **32 (4)**, 247-252 (2007)
7. Łapka W., Cempel C., Computational and experimental investigations of a sound pressure level distribution at the outlet of the spiral duct, *Proceedings of the 55th Open Seminar on Acoustics*, Wrocław - Piechowice, Poland, 175-180 (2008)
8. Łapka W., Cempel C., Noise Reduction of Spiral Ducts, *International Journal of Occupational Safety and Ergonomics (JOSE)*, **13 (4)**, 419-426 (2007)
9. Łapka W., Cempel C., Acoustic attenuation performance of Helmholtz resonator and spiral duct, *Vibrations in Physical Systems*, **23**, 247-252 (2008)
10. Łapka W., Cempel C., Spiral waveguide and damper, *Proceedings of the 36th International Congress & Exhibition on Noise Control Engineering, Inter-Noise*, 191, 8 on CD, Istanbul, Turkey (2007)
11. Łapka W., Cempel C., Insertion loss of spiral acoustic duct – computational modeling, *Proceedings of the 35th Winter School on Vibroacoustical Hazards Suppressions*, 83-94, Wisła, Poland (2007)
12. COMSOL Multiphysics v. 3.4, Acoustic Module, COMSOL AB, www.comol.com, Stockholm, Sweden (2007)
13. Ingard U., On the theory and design of acoustic resonators, *Journal of the Acoustical Society of America*, **25**, 1037-1061 (1953)
14. Tang P. K., Sirignano W. A., Theory of generalized Helmholtz resonator, *Journal of Sound and Vibration*, **26**, 247-262 (1973)
15. Chanaud R. C., Effects of geometry on the resonance frequency of Helmholtz resonators, *Journal of Sound and Vibration*, **178**, 337-348 (1994)
16. Selamet A., Dickey N. S., Theoretical, computational and experimental investigation of Helmholtz resonators with fixed volume: lumped versus distributed analysis, *Journal of Sound and Vibration*, **187**, 358-367 (1995)
17. Givoli D., Neta B., High-oreder non-reflecting boundary scheme for time-dependant waves, J. Comp. Phys., **186**, 24-46 (2003)
18. Marburg S., Nolte B., *Computational Acoustics of Noise Propagation in Fluids – Finite and Boundary Element Methods*, 578, Springer-Verlag, Berlin, Germany (2008)

7. Acknowledgements

This work was supported by the Polish Ministry of Science and Higher Education, research project No. N N501289334.